ELSEVIER

Thermochimica Acta 400 (2003) 143–152

thermochimica acta

www.elsevier.com/locate/tca

Thermodynamic and structural analysis of the Pb–InSb system

Dusko Minic [a,*], Dragana Zivkovic [b], Zivan Zivkovic [b]

[a] *University of Pristina, Mining and Metallurgy Faculty, 38220 Kosovska Mitrovica, Yugoslavia*
[b] *University of Belgrade, Technical Faculty, 19210 Bor, Yugoslavia*

Received in revised form 30 July 2002; accepted 24 September 2002

Abstract

Results of thermodynamic and structural analysis of the Pb–InSb system are presented in this paper. Thermodynamic investigations were performed experimentally by Oelsen's calorimetric method and calculated by thermodynamic predicting according to Chou's general solution model, while structural analysis of the alloys in Pb–In–Sb system was done by SEM–EDX and diffractometry.

Keywords: Alloy thermodynamics; Pb–InSb system; Calorimetry; GSM; SEM–EDX; Diffractormetry

1. Introduction

Alloys in Pb–In–Sb ternary systems belongs to the group of lead alloys widely applied in different branches of industry [1–3]. Their thermodynamic and structural characteristics have not been investigated completely [4,5], although there are a lot of literature data on the constitutive binaries: Pb–In [6–10], In–Sb [11,12] and Sb–Pb [13–16], as well as references from Hultgren's book [17].

Considering the literature data on Pb–In–Sb ternary system thermodynamics, one should mention the paper of Geis and Peretti [4], who investigated different sections with different molar ratios of lead and indium, while Minic et al. [5] did the experimental research of thermodynamic properties of the section with molar ratio In:Sb = 0.3:0.7. As for the investigations of the structural characteristics of the alloys in the Pb–In–Sb system, there are also some references [18–22].

Section Pb–InSb in the mentioned ternary system, with molar ratio In:Sb = 1:1, was investigated in this paper in order to contribute to the better knowledge of its thermodynamic and structural characteristics.

2. Experimental

Metals lead, indium and antimony of p.a. purity were used for the experimental work. All experiments were carried out in an air atmosphere. Compositions of the investigated samples are given in Table 1.

Oelsen's calorimetry was used for the thermodynamic analysis of the investigated Pb–In–Sb system. Description of this experimental technique is reported in [23–25]. The water equivalent was determined by a standard method using dissolved Na_2CO_3 and for calorimeter used it had a value of 3314 J/°C. Also, according to the method used, volume of all samples (given in Table 1) was constant—1 cm^3.

SEM analysis was performed on Philips microscope XL-300 type with EDX of resolution of 1 nm on 30 kV and 5 nm on 1 kV, extinction voltage of 0.2–30 kV

* Corresponding author.
E-mail address: jmm@eunet.yu (D. Minic).

0040-6031/03/$ – see front matter
PII: S0040-6031(02)00490-2

Table 1
Compositions of the investigated samples

Samples	Mass (%)			X_i			m (g)			m (total)
	Pb	In	Sb	Pb	In	Sb	Pb	In	Sb	
U1	0	48.5353	51.4647	0	0.5	0.5	0	3.3837	3.5879	6.9716
U2	30.4545	33.7537	35.7909	0.2	0.4	0.4	2.4081	2.6689	2.83	7.907
U3	53.8703	22.3892	23.7405	0.4	0.3	0.3	4.7495	1.9739	2.0931	8.8165
U4	63.6588	17.6384	18.7028	0.5	0.25	0.25	5.8961	1.6336	1.7322	9.2619
U5	72.4332	13.3796	14.1872	0.6	0.2	0.2	7.0269	1.2979	1.3763	9.7011
U6	80.3432	9.5405	10.1163	0.7	0.15	0.15	8.1424	0.9668	1.0252	10.1344
U7	87.5106	6.0617	6.4277	0.8	0.1	0.1	9.2429	0.6402	0.6788	10.6005
U8	100	0	0	1.0	0	0	11.4	0	0	11.4

and magnification of 5 00 000×. Samples recorded by SEM were prepared by standard metallographic methodology.

Crystallographic investigations were done on diffractometer Philips Pw 1710. Selected samples, in a form of a metal plate and powder, were investigated under following conditions: copper anticathode with wavelength Cu Kα = 1.54178 Å; graphite monochromator with working voltage of 40 kV; current intensity of 30 mA. Samples were investigated in the range of 4–90° 2θ, with step of 0.02° and time delay of 0.8 s.

3. Theoretical fundamentals

Thermodynamic analysis of the investigated Pb–InSb system was done experimentally by Oelsen's

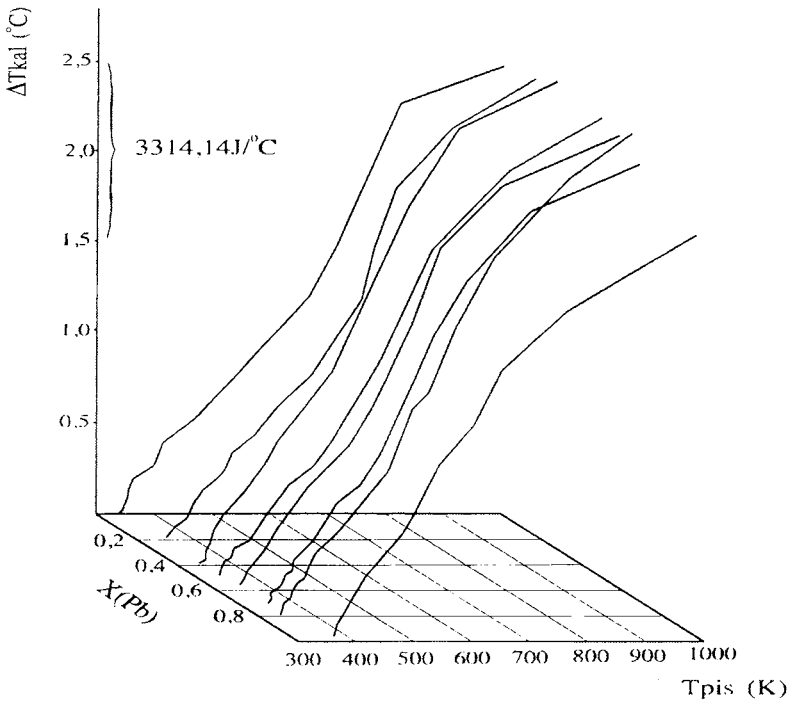

Fig. 1. Space enthalpy diagram.

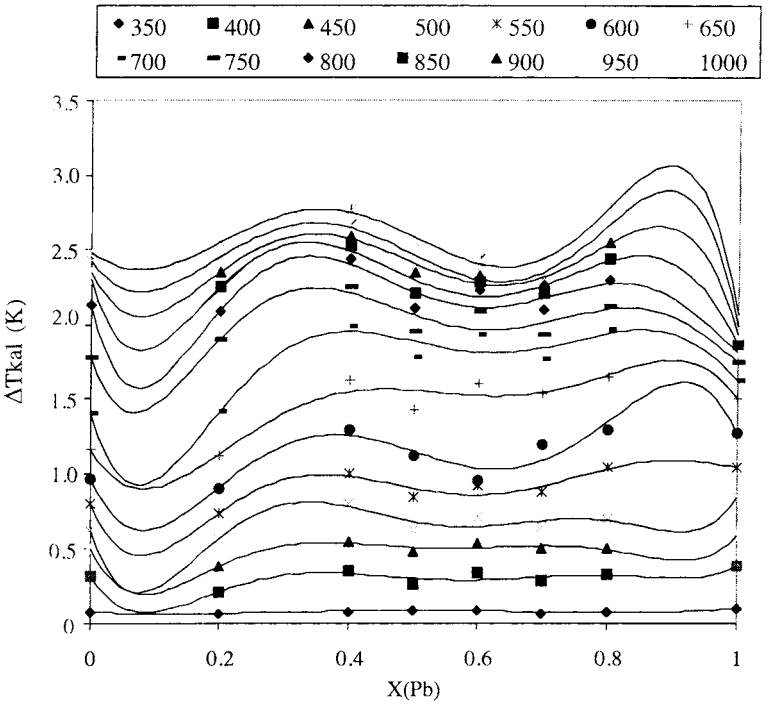

Fig. 2. Enthalpy isotherm diagram for the temperature interval 773–973 K.

calorimetry and analytically by thermodynamic predicting according to Chou's general solution model.

Basic equation of the quantitative thermodynamic analysis according to Oelsen's calorimetry is given as [22]

$$\frac{G_i^{\mathrm{M}}}{T} = \int_{1/T_0}^{1/T} H_{X,T}\,\mathrm{d}\left(\frac{1}{T}\right) = -R\ln a_i \qquad (1)$$

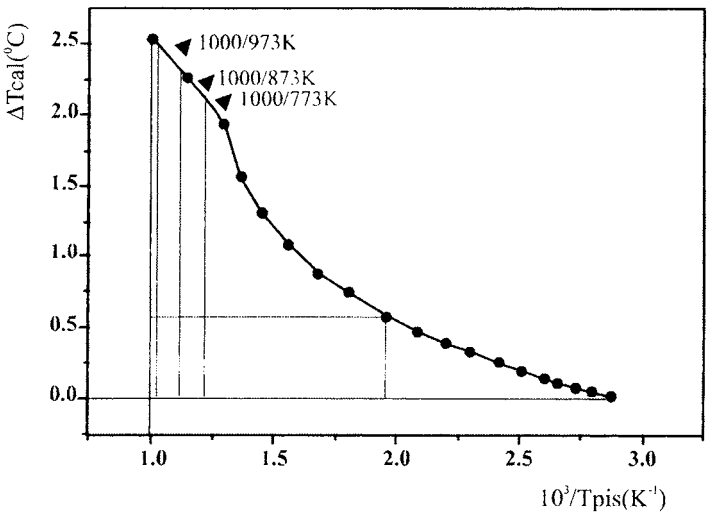

Fig. 3. Graphic planimetry (sample U2).

where G_i^{M} is the partial molar Gibbs energy for component i, T_0 the starting temperature, T the final temperature, $H_{X,T}$ the enthalpy value measured in the Oelsen's calorimeter for the temperature change from T_0 to T, R the gas constant and a_i is the activity of component i.

Considering Chou's general solution model for the predicting of thermodynamic properties in ternary systems, basic equations are given as follows [26,27]:

$$G^{\mathrm{E}} = x_1x_2(A_{12}^0 + A_{12}^1(x_1 - x_2) + A_{12}^2(x_1 - x_2)^2) + x_2x_3(A_{23}^0 + A_{23}^1(x_2 - x_3) + A_{23}^2(x_2 - x_3)^2) + x_3x_1(A_{23}^0 + A_{31}^1(x_3 - x_1) + A_{31}^2(x_3 - x_1)^2) + fx_1x_2x_3 \quad (2)$$

where A_{ij}^0, A_{ij}^1 and A_{ij}^2 are the parameters for binary system "ij" independent of composition, only relying on temperature, which have been used in the regular type equation

$$G_{ij}^{\mathrm{E}} = X_iX_j(A_{ij}^0 + A_{ij}^1(X_i - X_j) + A_{ij}^2(X_i - X_j)^2 + \cdots + A_{ij}^n(X_i - X_j)^2) \quad (3)$$

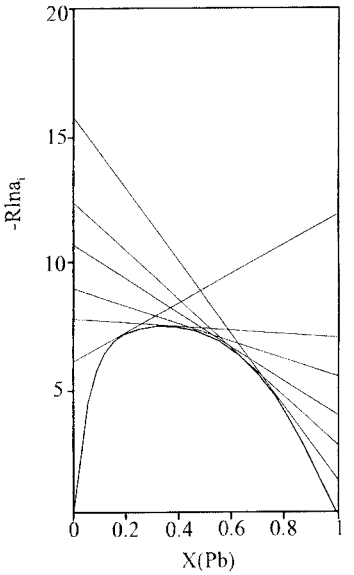

Fig. 4. Tangent construction for determination of $-\mathrm{R}\ln a_{X,T}$.

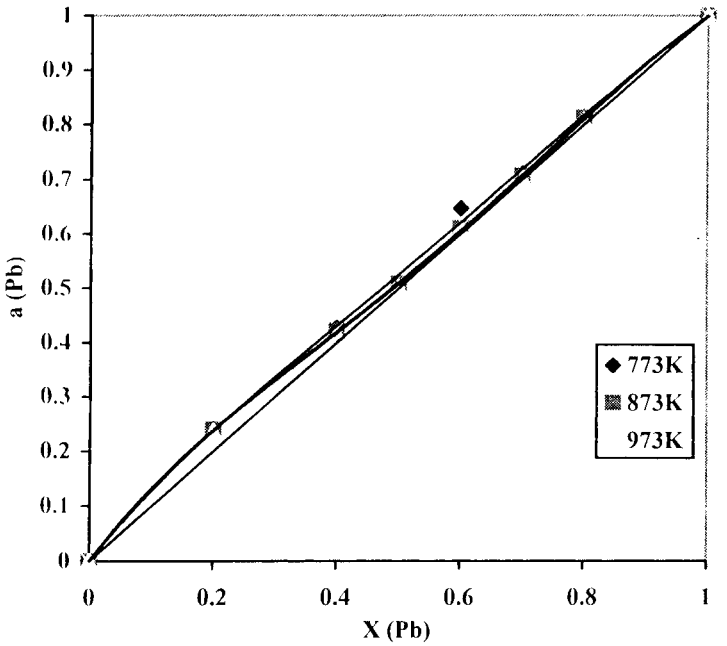

Fig. 5. Graphic presentation of dependence a_{Pb} vs. composition at 773, 873 and 973 K.

where X_i and X_j indicate the mole fraction of component "i" and "j" in "ij" binary system. The function f is the ternary interaction coefficient expressed by

$$f = (2\xi_{12}-1)\{A_{12}^2((2\xi_{12}-1)x_3 + 2(x_1-x_2)) + A_{12}^1\} + (2\xi_{23}-1)\{A_{23}^2((2\xi_{23}-1)x_1 + 2(x_2-x_3)) + A_{23}^1\} + (2\xi_{31}-1)\{A_{31}^2((2\xi_{31}-1)x_2 + 2(x_3-x_1)) + A_{31}^1\}, \quad (4)$$

where ξ_{ij} is the similarity coefficients defined by η_i called the deviation sum of squares

$$\xi_{ij} = \frac{\eta_i}{\eta_i + \eta_j} \quad (5)$$

where

$$\eta_{\mathrm{I}} = \int_{x_i=0}^{x_i=1} (\Delta G_{12}^{\mathrm{E}} - \Delta G_{13}^{\mathrm{E}})^2 \, \mathrm{d}X_1,$$
$$\eta_{\mathrm{II}} = \int_{x_i=0}^{x_i=1} (\Delta G_{21}^{\mathrm{E}} - \Delta G_{23}^{\mathrm{E}})^2 \, \mathrm{d}X_2,$$
$$\eta_{\mathrm{III}} = \int_{x_i=0}^{x_i=1} (\Delta G_{31}^{\mathrm{E}} - \Delta G_{32}^{\mathrm{E}})^2 \, \mathrm{d}X_3, \quad (6)$$

and

$$X_{1(12)} = x_1 + x_3\xi_{12}, \qquad X_{2(23)} = x_2 + x_1\xi_{23},$$
$$X_{3(31)} = x_3 + x_2\xi_{31} \quad (7)$$

In all given equations, G^{E} and G_{ij}^{E} correspond to the integral molar excess Gibbs energies for ternary and binary systems, respectively, while x_1, x_2, and x_3 correspond to the mole fraction of components in investigated ternary system.

4. Results and discussion

4.1. Thermodynamic analysis

According to Oelsen's thermodynamic analysis [22–24], temperature change of calorimeter was determined for all samples in the investigated temperature interval 773–973 K based on the cooling curves. Considering these data, the space enthalpy diagram the dependence of the temperature change of calorimeter on composition and temperature, and the enthalpy isotherm diagram were constructed. These diagrams are presented in Figs. 1 and 2, respectively.

Further step in the quantitative analysis was the graphic planimetry, Fig. 3, and finally, the tangent construction for determination of $-\mathrm{R}\ln a_{X,T}$, Fig. 4, which is done according to Eq. (1).

Considering the results of graphic planimetry, lead activities were determined at different temperatures—773, 873 and 973 K and shown in Fig. 5, while other calculated partial molar thermodynamic quantities for lead are given in Table 2.

Positive deviation from ideal behaviour is typical for this system at all investigated temperatures.

Activity coefficients for lead increase slightly with temperature decreasing, and their values are greater than 1 in the whole investigated concentration area. Partial molar quantities follow this trend, so $G_{\mathrm{Pb}}^{\mathrm{XS}}$ decreases as temperature decreases, and $G_{\mathrm{Pb}}^{\mathrm{M}}$ increases

Table 2
Results of Oelsen's thermodynamic analysis (energies in J/mol)

Samples	a (Pb)	γ (Pb)	G^{XS} (Pb)	G^{M} (Pb)
973 K				
U1	0	–	–	–
U2	0.2378	1.1895	1403.7	−11 615
U3	0.4167	1.0417	330.48	−7081
U4	0.502	1.004	32.29	−5574
U5	0.6105	1.0175	140.34	−3991
U6	0.7024	1.0034	27.45	−2857
U7	0.8072	1.009	72.48	−1732
U8	1	1	–	–
873 K				
U1	0	–	–	–
U2	0.2393	1.1965	1302.1	−10 379
U3	0.4206	1.0515	364.48	−6286
U4	0.5078	1.0156	112.35	−4918
U5	0.6113	1.0188	135.18	−3572
U6	0.7067	1.0095	68.622	−2519
U7	0.8124	1.0155	111.63	−1507
U8	1	1	–	–
773 K				
U1	0	–	–	–
U2	0.2413	1.2065	1206.4	−9136
U3	0.4269	1.067	416.7	−5470
U4	0.5103	1.0206	131.045	−4323
U5	0.6175	1.029	183.72	−3098
U6	0.7104	1.0148	94.418	−2197
U7	0.8145	1.018	114.65	−1318
U8	1	1	–	–

Table 3
Binary regular parameters and similarity coefficients at 973 K

Pb–ln (1–2)[a]			ln–Sb (2–3)[b]			Sb–Pb (3–1)[c]		
A_{12}^0	A_{12}^1	A_{12}^2	A_{23}^0	A_{23}^1	A_{23}^2	A_{31}^0	A_{31}^1	A_{31}^2
756.1544	−991.526	1257.713	−3799.73	6320.694	−370.019	−529.121	1043.995	−372.527

[a] $\xi_{12} = 0.05893$.
[b] $\xi_{23} = 0.762926$.
[c] $\xi_{31=}0.832281$.

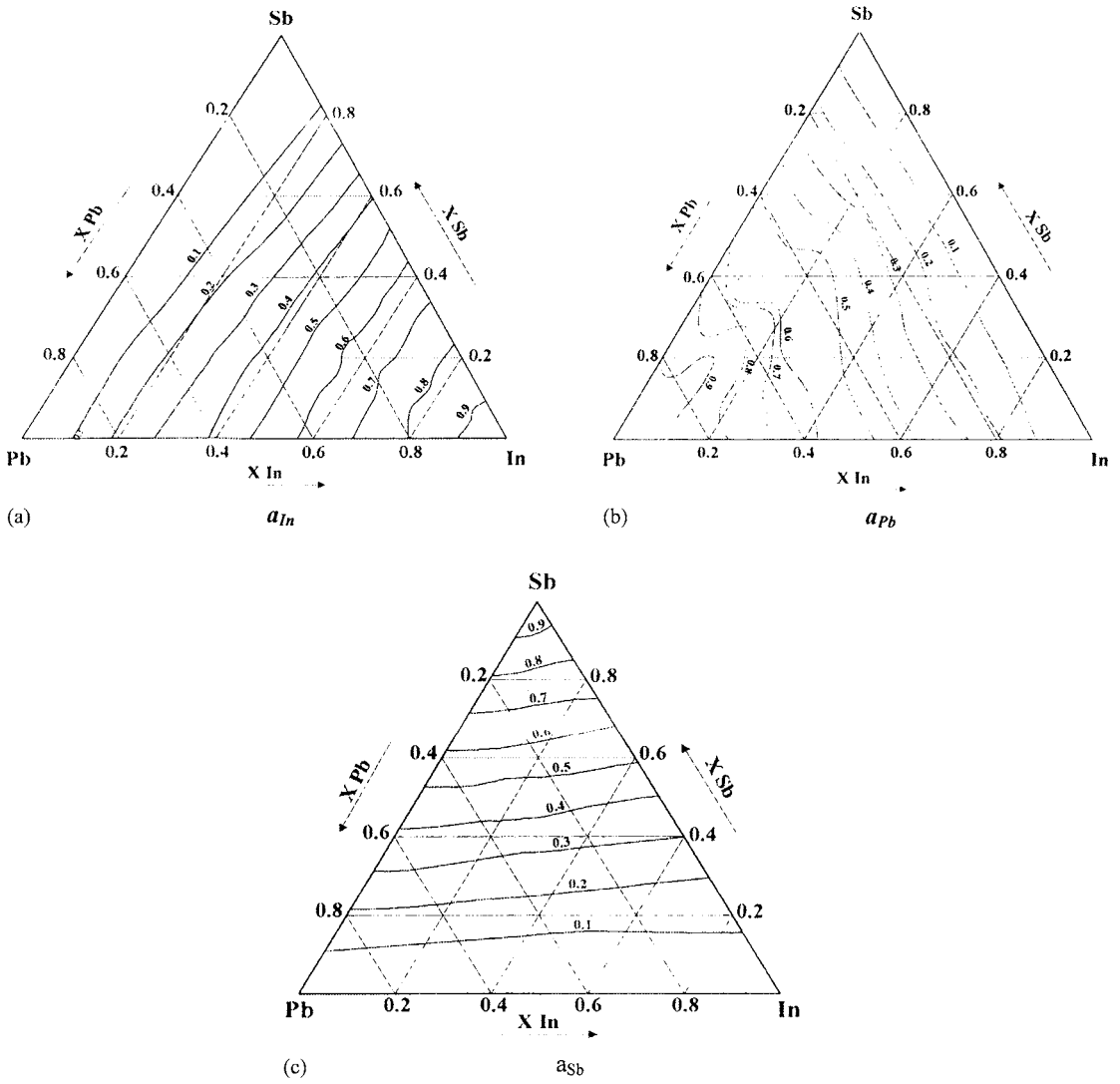

Fig. 6. Activities of the constituent elements in Pb–InSb system, shown at the iso-activity diagrams of the Pb–InSb system for temperature of 973 K.

as temperature decreases in the investigated temperature interval 773–973 K.

For the thermodynamic predicting according to Chou's general solution model, values for the integral molar excess Gibbs energies for the constituent binary systems Pb–In, In–Sb and Sb–Pb, available in the literature for the temperature of 973 K [17], were used as the starting data for the calculation. Their binary regular parameters were calculated firstly by Eq. (3) are presented in Table 3, and also, similarity coefficients for three constituent binary systems, calculated by Eqs. (5)–(7), are presented in the same table.

Based on these data and according to Eqs. (2) and (4), thermodynamic predicting was done for the selected alloys (Table 1) in the Pb–InSb system, and values of the integral molar excess Gibbs energies and ternary interaction coefficients were determined and shown in Table 4, while calculated activities for three constituent elements are presented (Fig. 6) at the iso-activity diagrams of the Pb–In–Sb ternary system [27].

Results obtained by thermodynamic predicting according to Chou's general solution model show that activity coefficients for in and Sb are smaller than 1, while activity coefficients for Pb are greater than 1. This indicates that indium and antimony possess affinity for mutual miscibility, according to fact that these elements form In–Sb intermetal compound. On the other hand, lead shows opposite behaviour and weanermiscibility with other two components of the system.

Table 4
Results of thermodynamic predicting according to Chou's general solution model (energies in J/mol)

	x (Pb)	f	ΔG^{XS}_{123}	a_{Pb}	a_{In}	a_{Sb}
L1	0	6035.2	−949.93	0	0.277	0.277
L2	0.1	5730.1	−606.254	0.126	0.286	0.286
L3	0.2	5425.0	−380.79	0.2294	0.289	0.289
L4	0.3	5120.0	−242.54	0.321	0.282	0.282
L5	0.4	4814.9	−164.75	0.409	0.265	0.265
L6	0.5	4509.8	−124.86	0.4986	0.236	0.236
L7	0.6	4204.7	−104.54	0.5916	0.197	0.197
L8	0.7	3899.7	−89.6707	0.69	0.149	0.149
L9	0.8	3594.6	−70.367	0.794	0.0972	0.0972
L10	0.9	4409.4	−158.29	0.885	0.0305	0.0305
L11	1	2984.4	0	1	0	0

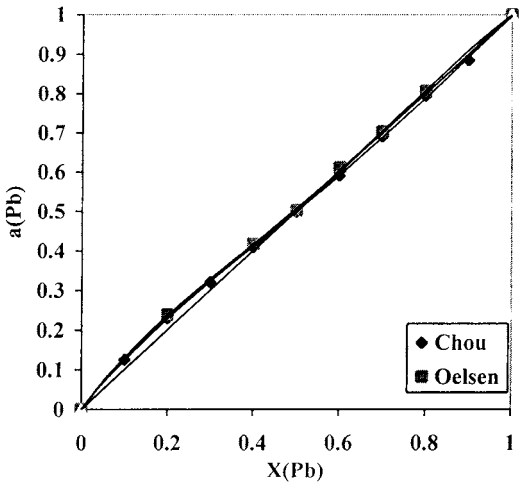

Fig. 7. Comparative review of lead activities at 973 K.

In order to present predicted thermodynamic values graphically iso-activity diagrams were constructed at temperature 973 K and show in Fig. 6.

Comparison of the experimentally obtained and predicted lead activities shows good agreement, as presented in Fig. 7. Also, positive deviation from Raoult's law is presented in the whole concentration area of the investigated Pb–InSb system, which indicates weaker miscibility of lead with In–Sb in the solution at given temperatures.

4.2. Structural analysis

Structural analysis was done for samples U2, U4 and U6 (compositions given in Table 1), by using SEM–EDX analysis and crystallographic investigations.

Characteristic SEM microstructures of investigated samples are presented in Fig. 8, while results of EDX analysis in noted points are given in Table 5.

Phases noticed in microstructure of sample U2 (Fig. 8a) are: white phase (point 1) that mostly reach on lead, grey (point 2); dark phase (3) based on indium and antimony, while lead content in dark phase is higher. For sample U4 (Fig. 8b), two phases were noticed—grey phase (point 2) consisting of high lead content and low indium content, and dark phase (point 1) in which indium and antimony are mostly present with extremely low content of lead. Sample

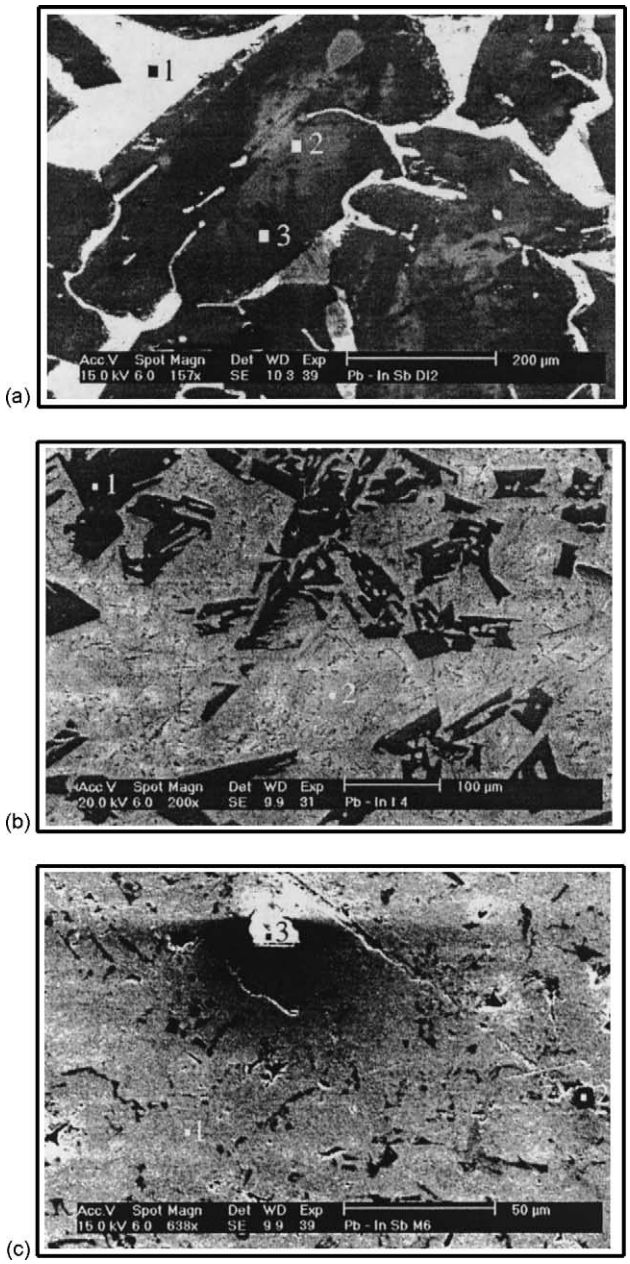

Fig. 8. SEM microstructures of samples U2 (a), U4 (b) and U6 (c).

U6 is characterised by following phases—grey (point 1) and dark phase (point 2) which contains lead, and almost equal contents of antimony and indium, and light phase (point 3) mostly reach on lead. Recorded diffractograms of the investigated samples are shown in Fig. 9.

Based on obtained relations between intensity values and interface distance, cell parameters and phases

Table 5
Results of EDX analysis in points noted at microstructures of investigated samples[a]

Samples	U2			U4		U6		
	Point 1	Point 2	Point 3	Point 1	Point 2	Point 1	Point 2	Point 3
Pb	45.7	3.74	14.72	2.56	96.34	45.7	22.02	81.24
In	27.72	48.3	43.08	50.37	3.66	27.7	39.99	8.37
Sb	26.57	47.96	42.2	47.06	–	26.6	37.99	10.39

[a] Values are compositions in at.%.

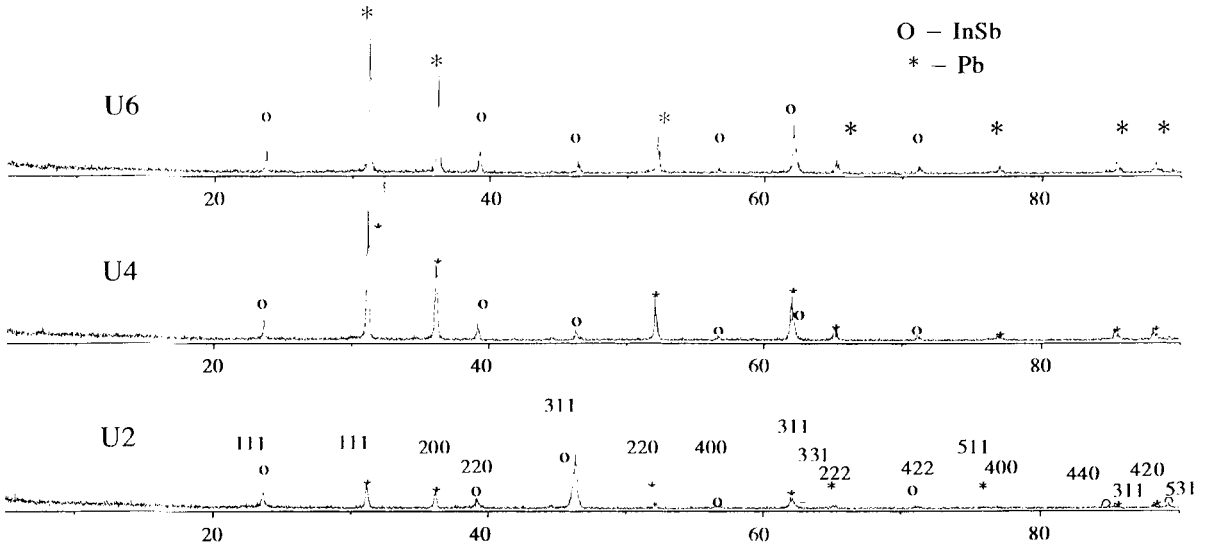

Fig. 9. Diffractograms of the investigated samples U2 (a), U4 (b), and U6 (c).

presented in the investigated samples were determined and shown in Table 6.

It can be concluded that two-phased alloys are characteristic for Pb–InSb system. Cubic, phase-centred lead and In–Sb of sphalerite (ZnS) structure are presented, with cell parameters of 4.964 and 6.489 Å, respectively. Crystal structure of In–Sb intermetal compound is shown in Fig. 10.

In In–Sb lattice, atoms create the most packed teseral structure, while antimony atoms fill one hale of available positions (space group $F4\text{-}3m$, $a = 6.4782$ Å at 25 °C, JCPDS-6-208, cell volume

Table 6
Results of crystallographic investigations

Samples	Phase compositions	Structure types	Contents of cell	Cell parameters a (Å)	Volumes V (Å^3)
U2	Pb, In–Sb	Pb	Pb_4	4.964(4)	122.3(3)
		In–Sb	In_4–Sb_4	6.489(3)	273.3(4)
U4	Pb, In–Sb	Pb	Pb_4	4.961(1)	122.1(1)
		In–Sb	In_4–Sb_4	6.4861(9)	272.9(1)
U6	Pb, In–Sb	Pb	Pb_4	4.961(1)	122.1(1)
		In–Sb	In_4–Sb_4	6.4861(9)	272.9(1)

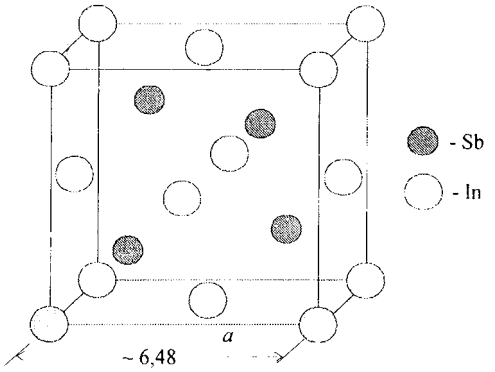

Fig. 10. Crystal structure of In–Sb intermetal compound.

271.87 Å^3). Indium coordinates are (0 0 0), (1/2 1/2 0), (1/2 0 1/2), (0 1/2 1/2), and for antimony (1/4 1/4 1/4), (1/4 3/4 3/4), (3/4 1/4 3/4), (3/4 3/4 1/4). Both atoms have the tetrahedra surrounded, by four atoms of In–Sb in cell.

5. Conclusions

Results of thermodynamic (calorimetric studies and GSM thermodynamic predicting) and structural (SEM–EDX and crystallography) investigations of alloys in Pb–InSb system are presented in this paper. Weak interactions of lead with other components could be noticed through positive deviation from Raoult's law according to thermodynamic analysis, which also show good mutual agreement between two used methods. Structural investigations confirm that alloys in the investigated system are two-phased, one phase is based on lead, and the other is based on In–Sb.

References

[1] R. Jayaganthan, J.P. Hajra, Met. Mater. Trans. A 29 (1998) 611.
[2] M.J. Krane, F.P. Incropera, D.R. Gaskell, Met. Mater. Trans. A 29 (1998) 843.
[3] W. Hofman, Lead and Lead Alloys, McGraw Hill, New York, 1970.
[4] D.R. Geis, E.A. Peretti, J. Chem. Eng. Data 8(3) (1963) 470.
[5] D. Minic, D. Zivkovic, Z. Zivkovic, J. Min. Met. B 36 (3–4) (2000) 169.
[6] P.J. Nabot, I. Ansara, Bull. Alloy Phase Diag. 8 (3) (1987) 246.
[7] E. Scheil, L.H. Lukas, Z. Metallknd. 52 (6) (1961) 417.
[8] D. Minic, D. Zivkovic, Z. Zivkovic, Thermochim. Acta 372 (2001) 85.
[9] A. Bolcavage, C.G. Rao, S.L. Chon, Y.A. Chang, in: P. Nash, B. Sundman (Eds.), Proceedings of the Symposium on Application of Thermodynamics in the Synthesis and Processing of Materials, 1995, TMS, Warendale, Pa, p. 171.
[10] D. Boa, I. Ansara, Thermochim. Acta 314 (1998) 79.
[11] I.V. Kashin, M.A. Katsnelsin, S.A. Krylov, J. Phase Eq. 13 (5) (1992) 578.
[12] A. Schneider, H. Klotz, Naturwuss. 46 (1959) 141.
[13] N.V. Eremenko, M.O. Eremenko, Khim. Zhur. 18 (2) (1952) 232.
[14] B. Blumenthal, Mini. Met. Eng. 152 (1943) 65.
[15] S. Pelini, N.F. Rhines, Min. Met. Eng. 152 (1943) 65.
[16] H. Seltz, B.J. Witt, J. Am. Chem. Soc. 61 (1939) 2594.
[17] R. Hultgren, et al., Selected Values of Thermodynamic Properties of Metals and Alloys, Wiley, New York, 1963.
[18] A. Hideki, V. Minagava, N. Katsuyoshi, in: Proceedings of the TMS Annual Meeting Exhibition, Texas, 1998.
[19] G. Raynor, J. Graham, Trans. Faraday Soc. 54 (1958) 161.
[20] G. Ozolin, K. Averkjeva, N. Gorjunova, A. Levins, Kristalografia 8 (1963) 272.
[21] C. Jordan, J. Chem. Phys. 39 (1963) 1613.
[22] W. Oelsen, Arch. Eisenhuttenwess. 26 (1955) 519.
[23] W. Oelsen, E. Schurmann, H.J. Weigt, O. Oelsen, Arch. Eisenhuttenwess. 27 (1956) 487.
[24] W. Oelsen, F. Bieret, G. Schwebe, Arch. Eisenhuttenwess. 27 (1956) 607.
[25] K.C. Chou, CALPHAD 19 (3) (1995) 315.
[26] K.C. Chou, W.C. Li, F. Li, M. He, CALPHAD 20 (1996) 395.
[27] D. Minic, Doctoral Dissertation, University of Belgrade, Technical Faculty, Bor, Yugoslavia.